can be studied in vivo, but there have been too few studies of the physiological interactions between endothelial and smooth muscle cells in the intact arteriole to permit conclusions regarding the role of gap junctions in propagated vasodilation.

REFERENCES AND NOTES

1. D. D. Stromberg and J. R. Fox, *Circ. Res.* **31**, 229 (1972); H. G. Bohlen, R. W. Gore, P. M. Hutchins, *Microvasc. Res.* **13**, 125 (1977); H. G. Bohlen and R. W. Gore, *ibid.* **14**, 251 (1977); S. H. Nellis, A. J. Liedtke, L. Whitesell, *Circ. Res.* **49**, 342 (1981); S. S. Segal and B. R. Duling, *ibid.* **59**, 283 (1986).
2. R. Ingebrigtsen and S. Leraand, *Acta Physiol. Scand.* **79**, 552 (1970); M. Lie, O. M. Sejersted, F. Kiil, *Circ. Res.* **27**, 727 (1970).
3. J. Holtz *et al.*, *Z. Kardiol.* **72**, 98 (1983).
4. B. R. Duling and R. M. Berne, *Circ. Res.* **26**, 163
5. A. Krogh, G. A. Harrop, P. B. Rehberg, *J. Physiol. (London)* **56**, 179 (1922); B. R. Lutz, G. P. Fulton, R. P. Akers, *Exp. Med. Surg.* **8**, 258 (1950); S. S. Segal and B. R. Duling, present observations.
6. D. M. Larson, E. Y. Kam, J. D. Sheridan, *J. Membrane Biol.* **74**, 103 (1983).
7. F. Mekata, *J. Physiol. (London)* **242**, 143 (1974). S. M. Hilton proposed that a vasodilatory stimulus could be conducted along the blood vessel wall [*ibid.* **149**, 93 (1959)].
8. Male hamsters (120 g) were anesthetized with sodium pentobarbital; cheek pouches were prepared for observation of microvessels [B. R. Duling, *Microvasc. Res.* **5**, 423 (1973)]. Esophageal and cheek pouch temperatures were maintained at 37°C. Cheek pouch preparations were superfused continually with a bicarbonate-buffered physiological salt solution (*p*H 7.4) equilibrated with 5% CO_2 and 95% N_2 during free-flow conditions. Glass micropipettes, beveled to an internal tip diameter of 2 μm, were filled with 1.0*M* acetylcholine chloride (Sigma) dissolved in distilled water. The micropipette tip was positioned 4 to 6 μm from the arteriolar wall, and ACh was applied via an iontophoresis programmer (World Precision Instruments, model 160). The retaining current, typically 100 nA, was established as the minimum required to prevent local dilation due to ACh leakage from the pipette tip. Ejection currents were typically 200 msec in duration and 1000 nA in amplitude. Sodium chloride (1.0*M*) was prepared and iontophoresed in a similar fashion as a control. Microvessels were observed by videomicroscopy with transmitted light at a magnification of ×1200. Vessel diameters were recorded continuously with a video analyzer (Colorado 321), the output of which was directed to a chart recorder. To eliminate the potential for convective transport of ACh in arteriolar blood, we observed sites upstream from the point of ACh application. Countercurrent transport of ACh was circumvented either by simultaneous occlusion of adjacent venules or by observing arteriole segments devoid of adjacent venules.
9. The dilation induced by acetylcholine propagates upstream into larger arterioles (diameter, 40 to 60 μm). We have observed propagated vasodilation more than 3700 μm upstream from the stimulus origin.
10. According to the relation $t = \Delta x^2/2D$, where t is time, x is distance, and D is the diffusion coefficient [M. Jacobs, *Ergeb. Biol.* **12**, 1 (1935)], for $D = 10^{-5}$ cm^2/sec (approximate diffusion coefficient for small monovalent cations), diffusion of ACh or a chemical intermediate would require 5 seconds to move 100 μm and 500 seconds to move 1000 μm.
11. The response of arterioles to a vasoactive stimulus varies substantially as a function of vasomotor state. [R. W. Gore, *Am. J. Physiol.* **222**, 82 (1972)]. In control experiments performed during flow, we have observed that the vasoconstriction occurring in response to elevated oxygen did not qualitatively affect propagated vasodilation.
12. At 1029 ± 44 μm (mean ± SEM; $n = 4$) upstream from the ACh pipette, the amplitude of the propagated vasodilation both during flow and during double occlusion was 5.5 ± 0.9 μm; the length of occluded segments was 424 ± 56 μm.
13. For these experiments, a light-emitting diode (LED) was connected in series with the output of the iontophoresis unit and placed at the edge of the optical path to the video camera. In this configuration, the LED flash coincided with the iontophoretic stimulus. Video recordings were obtained of vascular responses adjacent to the micropipette and at measured increments along a vessel. Each video record contained the LED flash and a video timer signal accurate to hundredths of a second. Subsequently, the video record was played back frame by frame, and the interval between the LED flash and the onset of dilation was obtained. Propagation velocity was calculated by subtracting the interval determined at the pipette tip from similar intervals obtained at upstream locations.
14. With video analysis, we estimate that we could discern any delay exceeding 500 msec for the onset of dilation between two locations separated by a distance of 1 mm.
15. There is extensive documentation for both adrenergic and cholinergic arteriolar innervation: B. R. Lutz, G. P. Fulton, R. P. Akers, *Exp. Med. Surg.* **8**, 258 (1950); E. A. Schenk and A. E. Badawi, *Z. Zellforschung* **91**, 170 (1968); G. R. Siggins and H. A. Weitsen, *Microvasc. Res.* **3**, 308 (1971); W. L. Joyner, G. T. Campbell, C. Peterson, J. Wagoner, *ibid.* **26**, 27 (1983). Postganglionic neurons intrinsic to the arteriolar wall have been proposed to mediate vasodilation [H. A. Myers, E. A. Schenk, C. R. Honig, *Am. J. Physiol.* **229**, 126 (1975); C. R. Honig and J. L. Frierson, *ibid.* **230**, 493 (1976)]. In preliminary experiments, we have observed that 10^{-6}*M* tetrodotoxin did not affect the ACh-induced propagated vasodilation.
16. S. S. Segal and B. R. Duling, unpublished observations. Over 90% of the vessels examined demonstrated propagated vasodilation in response to an ACh stimulus. Both local and propagated vasodilation are blocked with 10^{-6}*M* atropine in the superfusate.
17. R. F. Furchgott and J. V. Zawadzki, *Nature (London)* **288**, 373 (1980).
18. N. B. Gilula, O. R. Reeves, A. Steinbach, *ibid.* **235**, 262 (1972); J. D. Pitts and J. W. Simms, *Exp. Cell Res.* **104**, 153 (1977); D. C. Spray, R. L. White, F. Mazet, M. V. L. Bennett, *Am. J. Physiol.* **248**, H753 (1985).
19. J. A. G. Rhodin, *J. Ultrastruct. Res.* **18**, 181 (1967); M. Simionescu, N. Simionescu, G. E. Palade, *J. Cell Biol.* **67**, 863 (1975); R. Taugner, H. Kirchheim, W. G. Forssmann, *Cell Tissue Res.* **235**, 319 (1984).

20. A preliminary report of these data was presented at the 1986 FASEB meetings. We thank D. N. Damon for his technical assistance and C. Desjardins for his critique of this manuscript. Supported by the NIH grants HL06947 and HL12792.

11 June 1986; accepted 23 September 1986

Vertical Nitrate Fluxes in the Oligotrophic Ocean

MARLON R. LEWIS, W. GLEN HARRISON, NEIL S. OAKEY, DAVID HEBERT, TREVOR PLATT

The vertical flux of nitrate across the thermocline in the upper ocean imposes a rigorous constraint on the rate of export of organic carbon from the surface layer of the sea. This export is the primary means by which the oceans can serve as a sink for atmospheric carbon dioxide. For the oligotrophic open ocean regions, which make up more than 75% of the world's ocean, the rate of export is currently uncertain by an order of magnitude. For most of the year, the vertical flux of nitrate is that due to vertical turbulent transport of deep water rich in nitrate into the relatively impoverished surface layer. Direct measurements of rates of turbulent kinetic energy dissipation, coupled with highly resolved vertical profiles of nitrate and density in the oligotrophic eastern Atlantic showed that the rate of transport, averaged over 2 weeks, was 0.14 (0.002 to 0.89, 95% confidence interval) millimole of nitrate per square meter per day and was statistically no different from the integrated rate of nitrate uptake as measured by incorporation of ^{15}N-labeled nitrate. The stoichiometrically equivalent loss of carbon from the upper ocean, which is the relevant quantity for the carbon dioxide and climate question, is then fixed at 0.90 (0.01 to 5.70) millimole of carbon per square meter per day. These rates are much lower than recent estimates based on in situ changes in oxygen over annual scales; they are consistent with a biologically unproductive oligotrophic ocean.

IN CONTEMPORARY, GLOBAL, GEOchemical models of the atmosphere-ocean carbon cycle, the oceans are viewed as the primary sink for atmospheric carbon dioxide (*1*). The responsible mechanism is the photosynthetic incorporation of dissolved carbon dioxide by marine microalgae in the upper ocean, followed by vertical loss of organic carbon, either through sinking particles or associated with vertical fluid transport. For the open ocean regions, which make up more than 75% of the world's oceans, both the rate of photosynthetic incorporation (the so-called total production) and the rate of export of organic carbon ("new" production) are currently uncertain to within an order of magnitude (*2*). Given the profound importance of the oceans in the global carbon cycle, this uncertainty propagates to a much greater uncertainty in prediction of future atmospheric carbon dioxide concentrations and hence in

M. R. Lewis and D. Hebert, Department of Oceanography, Dalhousie University, Halifax, Nova Scotia, B3H 4J1 Canada.
W. G. Harrison and T. Platt, Department of Fisheries and Oceans, Marine Ecology Laboratory, Bedford Institute of Oceanography, Dartmouth, Nova Scotia, B2Y 4A2 Canada.
N. S. Oakey, Department of Fisheries and Oceans, Atlantic Oceanographic Laboratory, Bedford Institute of Oceanography, Dartmouth, Nova Scotia, B2Y 4A2 Canada.

the prediction of the future climate of the earth.

For most of the world's oceans, nitrogen is the plant nutrient that limits the total production in the well-lit upper ocean (*3*). Therefore, the flux of nitrogen into the upper layer sets a rigorous constraint on the rate of export of carbon; over a suitable averaging time, these two fluxes must be in a stoichiometric balance set by the Redfield ratio (*4*) of 6.4 atoms of carbon per atom of nitrogen.

It is the vertical flux of nitrate from deep water rich in nutrient to the relatively impoverished surface layer that dominates the nitrate supply for most of the oligotrophic region. After surface heating stratifies the water column in early spring, most of the transport is associated with vertical turbulent fluid motions. The rate of turbulent mixing, and consequently the magnitude of the vertical flux of nitrate, has been extremely difficult to estimate in the past; recently, however, it has been made possible through direct measurements of microscale gradients in temperature and velocity shear fluctuations (*5*). We present the first measurements in any ocean region of rates of turbulent supply of nitrate to the surface layer and compare the results with direct measurement of the rate of incorporation of nitrate (as ^{15}N) by the resident algal population.

Experiments were carried out during a 2-week occupation of a station in the oligotrophic eastern Atlantic (28°30'N, 23°0'W). The site investigated is adjacent to the Beta triangle area (*6*) approximately 1000 km south-southeast of the Azores and corresponds to a "shadow" region in the eastern North Atlantic (*7*), where surface isopycnals do not close but intersect the coast and where nutrient concentrations are below the limit of detection along near-surface isopycnals (*8*). Hence, vertical diapycnal mixing is the dominant means by which nitrate is transported into the upper ocean.

The net upward flux of nitrate represents a source of nutrient which is available for local algal uptake. Assuming horizontal fluxes to be small in relation to vertical fluxes,

$$\frac{\partial N(z)}{\partial t} = \frac{\partial}{\partial z}K_v\frac{\partial N(z)}{\partial z} - [\alpha E_0 \exp(-k_s z)]\gamma N(z) \quad (1)$$

where the rate of change of local nitrate concentration [N(*z*)] depends on a balance between the turbulent supply (here described by a constant eddy diffusivity coefficient, K_v) and a sink in the form of algal uptake (*9*). The sink term is defined by a linear, light-dependent, total production (α is the initial slope of the photosynthesis-irradiance relation expressed in nitrogen equivalents, E_0 is the sea-surface photosynthetically active irradiance, and k_s is the optical attenuation coefficient) multiplied by the fraction of it that is satisfied by uptake of the oxidized nitrogen source, nitrate. This fraction, termed the *f*-ratio, is a linear function of local nitrate concentrations ($f = \gamma N$) in agreement with recent data (*10*). A time scale for biological uptake of nitrate in the euphotic zone is then $\tau_B = (\alpha E_0 \gamma)^{-1}$.

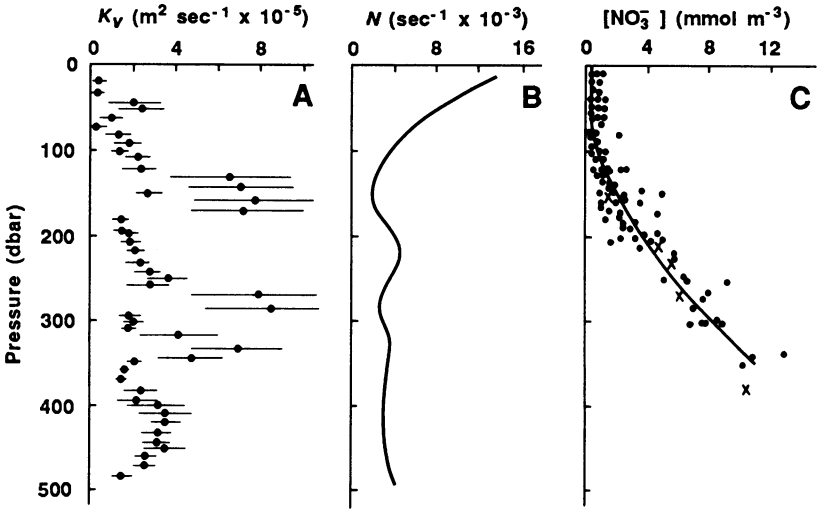

Fig. 1. Depth profiles (A) of eddy diffusivity, (B) buoyancy frequency, and (C) nitrate concentrations. Diffusivities are represented by 20-dbar averages calculated every 10 dbar, and the standard errors. For the nitrate profile, the solid line is the least-squares fit to Eq. 2. The x data points are from the GEOSECS expedition (*8*) in March.

If one assumes a local balance between the two terms on the right hand side of Eq. 1, the vertical profile of nitrate concentration is

$$\frac{N(z)}{N(0)} = \frac{K_1(\beta)I_0(\xi) + I_1(\beta)K_0(\xi)}{K_1(\beta)I_0(\beta) + I_1(\beta)K_0(\beta)} \quad (2)$$

with

$$\xi = \beta \exp(-z^*/2) \quad (3)$$

where I_i and K_i are modified Bessel functions of order *i*, β^2 is 4 $(\tau_B k_s^2 K_v)^{-1}$, the ratio of the time scale for biological nitrate uptake to that for mixing over one optical length scale, k_s^{-1}, and z^* is the depth normalized to the optical length scale. The assumption that the local time rate of change in nitrate concentration is small over the depth horizons of interest is supported by comparison of our measured nitrate profile, taken in June, with data from the Geochemical Ocean Sections Study (GEOSECS) (*8*) expedition at this station in early March (Fig. 1). The nitrate profiles are identical to 350 dbar. If one can constrain β and z^* by direct measurement of turbulence and optical properties, the biological rate of uptake, and hence the exported carbon, can be determined from the measured nitrate profile.

The rate of turbulent kinetic energy dissipation, ϵ, was determined from repeated measurements of microscale velocity shear fluctuations. The rates were very low (ensemble mean $\epsilon = 1.7 \times 10^{-9}$ m^2 sec^{-3}) and were distributed approximately log-normally with a standard deviation of 0.57 ($\log_{10}$ transform), a magnitude and distribution consistent with other recent measurements in the open ocean (*11*). On the basis of energetic arguments (*12*), as well as empirical measurements (*13*), the eddy diffusivity can be estimated from rates of turbulent kinetic energy dissipation and the buoyancy frequency, *N* (Fig. 1).

The optical properties were those of the clearest ocean water. The attenuation coefficient for downwelling irradiance was 0.037 (±0.005) m^{-1}, as determined from a new, free-fall irradiance sensor, and mean sea-surface irradiance during the occupation period was 720 μE m^{-2} sec^{-1} (λ = 400 to 700 nm only). Error limits are the standard error of the coefficients unless otherwise stated.

Equation 2 was fitted by nonlinear least-squares parameter estimation to highly resolved measurements of nitrate in the vertical (Fig. 1). Fitted parameter values were β = 11.8 (±0.8) (dimensionless) and N(0) = 1.4 (±1.2) × 10^{-5} mmol m^{-3}; with measured values of the attenuation coefficient and eddy diffusivity, the rate constant which sets the scale for the biological removal of nitrate (and carbon export) is then 1.5 × 10^{-6} sec^{-1}.

Direct measurements of nitrate and ammonium uptake were also made (*10*). Uptake of nitrate and ammonium showed distinct uncoupling in the vertical, with the peak in ammonium uptake (60 dbar) shallower than that of nitrate uptake (120 dbar; Fig. 2). These measurements from the oligotrophic Atlantic support the form of the

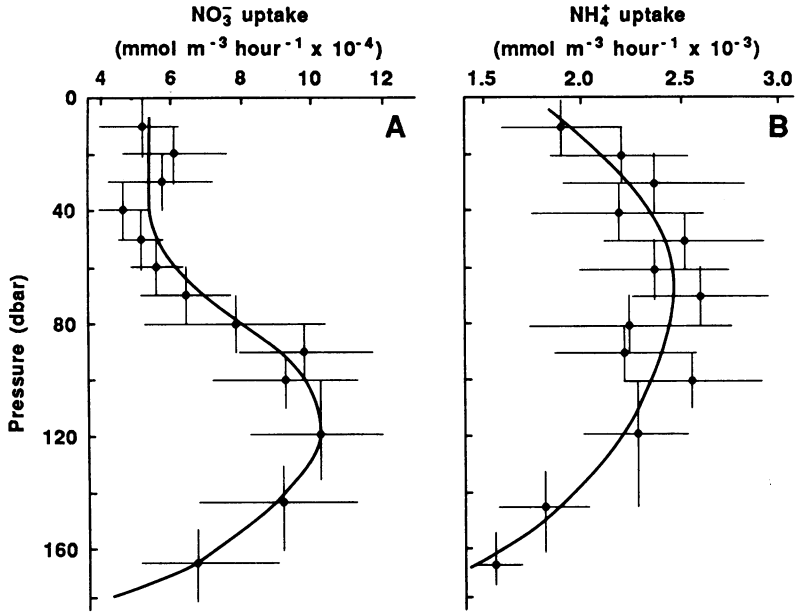

Fig. 2. Depth profiles of rate of uptake of nitrate and ammonium as ^{15}N. The vertical bars represent the range of the depth bin and the horizontal bars the standard error of the mean.

empirical relation between the *f*-ratio and ambient nitrate concentration established by Platt and Harrison (*10*) for coastal waters; the slope of the relation at low nitrate concentration is lower here however [γ = 0.74 ($\pm$0.18) m^3 $mmol^{-1}$], than in the previous study [γ = 5.48 ($\pm$0.77) m^3 $mmol^{-1}$].

The areal rate of new production can be calculated by substituting Eq. 2 into the second term on the right hand side of Eq. 1 and integrating from the sea surface to infinity: it is equivalent to the limiting value of the derivative of Eq. 2 with respect to depth (as $z \rightarrow \infty$) multiplied by the coefficient of eddy diffusivity. With dN/dz = 0.045 ($\pm$0.008) mmol m^{-4}, and the mean (100 to 400 dbar) measured $K_v = 3.7 \times 10^{-5}$ (6.1×10^{-7} to 2.3×10^{-4}, 95% confidence interval) m^2 sec^{-1}, the rate of new production is 0.14 (0.002 to 0.89, 95% confidence interval) mmol of nitrogen per square meter per day. For comparison, the measured integral nitrate uptake (as ^{15}N) is 0.807 ($\pm$0.17) mmol m^{-2} day^{-1} (180 dbar limit, Fig. 2), which is higher but not significantly different from the new production calculated from physical transport alone. We note that one-third of this 'new' production occurs below the conventional euphotic zone (125 m), set by the transmittance of 1% of the sea-surface irradiance.

If these results are shown to be representative, the implications for the global flux of carbon out of the surface regions of the world's oceans are profound. Over a suitable averaging period, this loss of carbon from the euphotic zone must be equivalent in a stoichiometric sense to the supply of nitrate (*2, 3*). With a Redfield ratio of 6.4, the inferred loss of carbon is less than 1 mmol m^{-2} day^{-1}. Evidence that these are indeed representative figures for the subtropical gyre is found from microstructure measurements in the gyral systems from both Atlantic and Pacific (*11*), where K_v values are 10^{-6} to 10^{-5} m^2 sec^{-1}, and where the nitrate gradient is very similar to that calculated here. Salt fingering may enhance the vertical mass flux (*14*), but the critical ratio of the gradients in salt and heat is not reached over most of the depth horizons of interest and no thermohaline staircases were observed in the temperature and salinity profiles (2-dbar resolution). Inertial oscillations may produce shear-induced instabilities which result in local intense mixing (*15*), but such processes would have been averaged and included in the data presented here.

It has been suggested that observed changes in chemical tracer concentrations such as ^3H, ^3He, and O_2, in water masses isolated from the sea surface, are more consistent with an average rate of new production of 2.5 mmol of nitrogen per square meter per day (15 mmol of carbon per square meter per day) (*16*), a result clearly outside the confidence bounds of the data presented here. We note that such methods yield results valid on an averaging scale of at least 1 year, whereas our results apply on a much shorter time scale. However, even if the mean eddy diffusivity were 10^{-4} m^2 sec^{-1}, as inferred from the thermocline heat balance (*17*), it would still be difficult to supply enough new nitrogen to support a rate of new production of this magnitude. Results based on in situ tracer dynamics have been criticized on several grounds (*18*), but even taking these into account, it is still difficult to reconcile the two sets of figures. At least, however, we can now reject the hypothesis that vertical turbulent supply is sufficient to meet the demands estimated from tracer dynamics. The only other sources of new nitrogen in the open ocean are from fixation of atmospheric nitrogen and import associated with acid rain. The rate of nitrogen fixation is currently thought to be several orders of magnitude less than the rate of supply by turbulent transport; the recent discovery of a new species of unicellular cyanobacteria capable of nitrogen fixation (*19*) and the difficulties of making the necessary measurements at sea (*20*) leaves open the possibility that this rate may be higher than previously thought.

Given the importance of the oceanic sink for global carbon flux models, and hence the prediction of future climate, it is imperative that this apparent discrepancy be resolved. For example, reassessment of the rate of production in the equatorial upwelling, coupled with new data on the *f*-ratio, recently led to an increase in the estimated annual new production in this region of 1.4 gigatons of carbon per year (*21*), a value which represents 25% of the annual atmospheric CO_2 discharge from fossil fuel combustion. The intermittency which characterizes both physical and biological processes in the ocean implies that advances in understanding will result only when adequate synoptic measurements of the processes that influence the rate of new production in the world's oceans are available (*22*).

REFERENCES AND NOTES

1. J. L. Sarmiento and J. R. Toggweiler, *Nature (London)* **308**, 621 (1984).
2. R. W. Eppley, in *Primary Productivity in the Sea*, P. G. Falkowski, Ed. (Plenum, New York, 1980), pp. 231–242; E. Shulenberger and J. L. Reid, *Deep Sea Res.* **28**, 901 (1981); W. J. Jenkins, *Nature (London)* **300**, 246 (1982); T. Platt, M. Lewis, R. Geider, in *Flows of Energy and Materials in Marine Ecosystems*, M. J. R. Fasham, Ed. (Plenum, New York, 1984), pp. 49–84; W. J. Jenkins and J. C. Goldman, *J. Mar. Res.* **43**, 465 (1985); T. Platt and W. G. Harrison, *Nature (London)* **318**, 55 (1985); J. L. Reid and E. Shulenberger, *Deep Sea Res.*, in press; T. Platt and W. G. Harrison, *ibid.*; T. Platt *et al.*, in preparation.
3. R. W. Eppley and B. J. Peterson, *Nature (London)* **282**, 677 (1979); P. M. Gilbert, in *Nitrogen Cycling in Coastal Marine Environments*, T. H. Blackburn and J. Sorensen, Eds. (Wiley, New York, in press).
4. A. C. Redfield, B. H. Ketchum, F. A. Richards, in *The Sea*, M. N. Hill, Ed. (Interscience, New York, 1963), pp. 26–77; T. Takahashi, W. S. Broecker, S. Langer, *J. Geophys. Res.* **90**, 6907 (1985).
5. T. R. Osborn and C. Cox, *Geophys. Fluid Dyn.* **3**, 321 (1972); T. Osborn, *J. Phys. Oceanogr.* **4**, 109 (1974); N. S. Oakey and J. A. Elliott, *ibid.* **12**, 171 (1982); M. R. Lewis *et al.*, *Nature (London)* **311**, 49 (1984).
6. W. J. Jenkins, *J. Phys. Oceanogr.*, in press.
7. J. L. Sarmiento, C. G. H. Rooth, W. Roether, *J. Geophys. Res.* **87**, 8047 (1982).
8. E. Bainbridge, *GEOSECS Atlantic: Hydrographic*

Data (Government Printing Office, Washington, DC, 1981), vol. 1.
9. R. W. Eppley, E. H. Renger, W. G. Harrison, *Limnol. Oceanogr.* **24**, 483 (1979); F. D. King and A. H. Devol, *ibid.*, p. 65 (1979); C. Garside, *Deep Sea Res.* **32**, 723 (1985).
10. W. G. Harrison, in *Nitrogen in the Marine Environment*, E. J. Carpenter and D. G. Capone, Eds. (Academic Press, New York, 1983).
11. M. C. Gregg, C. S. Cox, P. W. Hacker, *J. Phys. Oceanogr.* **3**, 458 (1973); A. E. Gargett, *ibid.* **6**, 139 (1976); M. C. Gregg and T. B. Sanford, *ibid.* **10**, 105 (1980). M. C. Gregg *et al.*, *Nature (London)* **318**, 140 (1985). R. Lueck and T. Osborn, *J. Geophys. Res.* **91**, 803 (1986).
12. T. R. Osborn, *J. Phys. Oceanogr.* **10**, 83 (1980).
13. N. S. Oakey, *ibid.* **12**, 256 (1982). N. S. Oakey, *ibid.* **15**, 1662 (1985).
14. R. Schmitt, *ibid.* **11**, 1015 (1981).
15. P. Klein and B. Coste, *Deep Sea Res.* **31**, 21 (1984).
16. E. Shulenberger and J. L. Reid, *ibid.* **28**, 901 (1981). W. J. Jenkins, *Nature (London)* **300**, 246 (1982); W. J. Jenkins and J. C. Goldman, *J. Mar. Res.* **43**, 465 (1985); W. J. Jenkins, *J. Phys. Oceanogr.*, in press. The required nitrogen flux of 2.5 mmol m^{-2} day^{-1} is calculated from data of W. J. Jenkins and J. C. Goldman [*J. Mar. Res.* **43**, 465 (1985)] with a new production rate of 4 mol of O_2 per meter squared per 150 days and an O_2:N ratio of 10.75 [T. Takahashi, W. S. Broecker, S. Langer, *J. Geophys. Res.* **90**, 6907 (1985)].
17. W. H. Munk, *Deep Sea Res.* **13**, 707 (1966); C. J. R. Garrett, *Dyn. Atm. Oceans* **3**, 239 (1979).
18. T. Platt, M. Lewis, R. Geider, in *Flows of Energy and Materials in Marine Ecosystems*, M. J. R. Fasham, Ed. (Plenum, New York, 1984), pp. 49–84; T. Platt, *Deep Sea Res.* **31**, 1311 (1984); ——— and W. G. Harrison, *ibid.*, in press.
19. J. Waterbury, *Can. J. Fish Aquatic Sci.*, in press.
20. L. A. Martinez, M. W. Silver, J. M. King, A. L. Alldredge, *Science* **221**, 152 (1983).
21. F. P. Chavez and R. T. Barber, *Eos* **66**, 1292 (1985).
22. O. B. Brown *et al.*, *Science* **229**, 163 (1985); National Academy of Sciences, *Global Ocean Flux Study* (National Academy Press, Washington, DC, 1984).
23. We thank A. Waite for assistance at sea, R. Palmer for chemical analyses, and C. J. R. Garrett for critical comments. Supported by operating grants from the Natural Sciences and Engineering Research Council (Canada) and by the Dalhousie University Research Development Fund.

9 June 1986; accepted 5 September 1986

Induction of Altered c-*src* Product During Neural Differentiation of Embryonal Carcinoma Cells

SALLY A. LYNCH, JOAN S. BRUGGE, J. M. LEVINE

The expression of the cellular *src* gene product pp60$^{c\text{-}src}$ was examined in an embryonal carcinoma cell line that differentiates in vitro into neuronlike cells after being treated with retinoic acid. Quantitative and qualitative changes in c-*src* expression accompanied the events associated with neuronal differentiation. The levels of pp60$^{c\text{-}src}$ increased 8- to 20-fold during the period when the cells elaborated neuritic processes and expressed neuron-specific proteins. The electrophoretic mobility of pp60$^{c\text{-}src}$ induced in these cells was retarded in comparison with that in untreated cells or in treated cells before neurite elaboration. The shift in electrophoretic mobility was due to an alteration in the amino terminal 16,000 daltons of pp60$^{c\text{-}src}$ and similar to an alteration of c-*src* protein found in neural tissues and in pure primary cultures of neuronal cells. These results indicate that expression of pp60$^{c\text{-}src}$ induced by retinoic acid in these embryonal carcinoma cells mimics the expression of c-*src* in developing neurons. Therefore, this embryonal carcinoma cell line provides a model system to investigate the function of the *src* protein in neuronal differentiation.

EMBRYONAL CARCINOMA (EC) CELL lines provide experimental models of the molecular events involved in cellular differentiation (*1*). EC cell lines develop from malignant stem cells present in teratocarcinomas and display morphological, biochemical, and biological properties of pluripotent cells of the early embryo (*2*). Murine EC cells can differentiate into a variety of cell types, depending on the conditions of cell culture. The nature of the cells that develop from stem cells is generally monitored on the basis of the morphology of the cells and of the expression of macromolecular markers specifically expressed in the differentiated cells (*3*). Although these markers are useful for classifying the differentiating cells, the analyses of these molecules do not provide insight into the events triggering cellular differentiation. Several lines of evidence implicate the normal cellular homologs of retroviral oncogenes (proto-oncogenes) as genes that might regulate cellular differentiation. Certain proto-oncogenes display patterns of expression specific to cell type; some actually encode growth factors or the receptors for growth factors that induce the proliferation of specific cells (*4*). In addition, experimental manipulation of the expression of the oncogenic homologs of these genes either stimulates differentiation of immature cells (*5, 6*) or interferes with the normal pathway of differentiation in cell culture (*7*).

One such proto-oncogene is c-*src*, the cellular homolog of the transforming gene of Rous sarcoma virus (RSV) (*8*). This proto-oncogene is one of several that encode tyrosine-specific protein kinases (*9*). Analysis of the c-*src* (pp60$^{c\text{-}src}$) protein during embryonic development has revealed both qualitative and quantitative differences in its pattern of tissue-specific expression (*10*). All neural tissues from developing embryos and adult animals contain high levels of a structurally distinct form of pp60$^{c\text{-}src}$ containing an alteration within the amino terminal region of the molecule (*11*). This novel form of pp60$^{c\text{-}src}$ was specifically expressed in primary cultures of pure neuronal cells and displayed a higher tyrosine kinase–specific activity than the protein expressed in astrocytic or fibroblastic cells (*12*). This pattern of expression suggests that the c-*src* protein may be important in either the differentiation of neurons or the events that take place in mature neurons. However, in the absence of a genetic system that provides the means to manipulate the expression of pp60$^{c\text{-}src}$, it is difficult to assess the role of pp60$^{c\text{-}src}$ in these events. Alemà and co-workers have shown that introducing the viral *src* protein into rat pheochromocytoma (PC12) cells stimulated the expression of a neuronal phenotype similar to that induced by nerve growth factor (NGF) (*5*). Although these results suggest a potential function for c-*src* in stimulating neuronal differentiation, it is difficult to correlate the functional behavior of the RSV pp60$^{v\text{-}src}$ protein with that of pp60$^{c\text{-}src}$ (*13*). Furthermore, PC12 cells may not be a useful system for analyzing the role of pp60$^{c\text{-}src}$ in normal differentiation, since no significant differences have been detected in the quantitative levels of pp60$^{c\text{-}src}$ or in its electrophoretic mobility after differentiation induced by NGF or cyclic adenosine monophosphate (*14*).

We have analyzed the expression of pp60$^{c\text{-}src}$ in an EC cell line, p19S18O1A1 (O1A1), that can be induced to differentiate into neuronlike cells under the influence of retinoic acid (*15*). We induced the O1A1 cells to differentiate by growing them as aggregates in retinoic acid, dissociating the aggregates into a single cell suspension, and plating the dissociated cells onto tissue culture plates coated with poly-L-lysine. Within 24 hours after plating, the cells began to elaborate neuritic processes, and after 3 to 5 days more than 80% of the cells could be labeled with antibodies to the neurofilament triplet polypeptides. This in vitro differentiation parallels the in vivo differentiation of

S. A. Lynch and J. S. Brugge, Department of Microbiology, State University of New York, Stony Brook, NY 11794.
J. M. Levine, Department of Neurobiology and Behavior, State University of New York, Stony Brook, NY 11794.